New York, 1986.
13. H. H. Schmidtke and D. Garthoff, *Inorg. Chim. Acta*, **2**, 357 (1968).
14. C. D. Flint and A. P. Matthews, *J. Chem. Soc. Faraday Trans. II*, **72**, 579 (1976).
15. K. W. Lee and P. E. Hoggard, *Transition Met. Chem.*, **16**, 377 (1991).
16. J. H. Choi, *Bull. Korean Chem. Soc.*, **14**, 118 (1993).
17. (a) A. D. Kirk and H. U. Güdel, *Inorg. Chem.*, **31**, 4564 (1992); (b) A. D. Kirk and D. Heyd, to be published.
18. P. E. Hoggard, *Inorg. Chem.*, **30**, 4644 (1991).
19. (a) M. J. D. Powell, *Computer J.*, **7**, 155 (1964); (b) J. L. Kuester and J. H. Mize, *Optimization Techniques with Fortran*, McGraw-Hill, New York, 1973.
20. A. A. Clifford, *Multivariate Error Analysis*, Wiley-Halsted, New York, 1973.
21. A. B. P. Lever, *Coord. Chem. Rev.*, **43**, 63 (1982).

Analysis of Steric Repulsion Forces in Atomic Force Microscope with Polyethylene Oxide in Aqueous Media

Sang Il Jeon* and Jeseph D. Andrade†

Department of Chemistry, Kangnung National University, Kangnung 210-702
†Departments of Bioengineering and Materials Science, University of Utah, Salt Lake City, Utah 84112, U.S.A., *Received October 27, 1992*

We present a theoretical analysis for the use of long-range intermolecular steric repulsion forces for imaging by atomic force microscope (AFM). Polyethylene oxide (PEO) is assumed to be terminally attaching to a spherical AFM tip in aqueous media. Only two long-range intermolecular forces (van der Waals attraction and steric repulsion) are considered. All calculated forces are near 10^{-11} N, which should not produce deformation of the soft protein surface. Calculations are presented as a function of surface density and chain length of terminally attached PEO, and other variables. Longer chain length and maximal surface density of terminally attached PEO to a smaller sized spherical AFM tip (modified AFM system) is appropriate to obtain optimum images of proteins on the surface.

Introduction

The atomic force microscope (AFM) can be used to obtain atomic scale images of observable surfaces[1-3]. The imaging contrast originates from intermolecular forces between the tip and the surface. The sample need not be a conductor to be imaged. The surfaces to be imaged can also be in an aqueous environment[3,4], which enables one to realistically image biological systems and monitor biological processes in real time. Most AFM research is performed in an air media[1,2,5,6] using short-range intermolecular forces[7,8]. Long-range intermolecular forces can reduce the risk of damage of the soft protein surface. Long-range intermolecular forces that have been utilized with the AFM are van der Waals force[9] in air and van der Waals and electrostatic forces[10] in aqueous media.

Polymers attached on solid surfaces immersed in a liquid medium are protected against aggregation by steric stabilization[11,12]. There exist long-range steric repulsion forces between two surfaces bearing such adsorbed polymer layers. These repulsive forces often exceed the long-range van der Waals and electrostatic forces acting between the bare surfaces[9]. Polyethylene oxide (PEO) surfaces are becoming recognized as exhibiting strongly reduced protein adsorption[14-20]. The protein-resistant character of PEO is generally recognized as a steric stabilization effect. The origin of these repulsive forces is attributed to two components[21-23]: the osmotic and elastic components. The osmotic component arises from the local increase in chain segment concentration upon compression resulting in the development of an osmotic pressure. The elastic component arises from the chain segments that have a tendency to extend themselves upon compression.

PEO can be attached to AFM tips of different sizes. The attached PEO can vary in molecular weight (chain length) and in number of chains per unit surface area (surface density), the 2 major molecular factors in steric repulsion[19,20]. In this paper we present a qualitative theoretical analysis of the steric repulsion forces of PEO attached to a spherical AFM tip interacting with a soft protein sample surface as a function of the surface density and chain length of PEO with the variation of the sizes of tip and sample surface.

Modeling

The shape of the tip is pyramidal and terminates in a point; the apex of the pyramid is approximated as a sphere[24]. PEO is assumed to be a neutral homopolymer with linear and flexible chains terminally attached to a spherical AFM tip (Figure 1(a)). The surface is assumed to be a hypothetical cylindrical protein adsorbed on mica. Although there can be various cylindrical shapes on the surface, only one unique cylindrical surface is considered (Figures 1(a)). It has a shape of circle from a top view. The surface is treated as one circle because that the assumed cylindrical surface is positioned under the PEO attached AFM tip and we consider

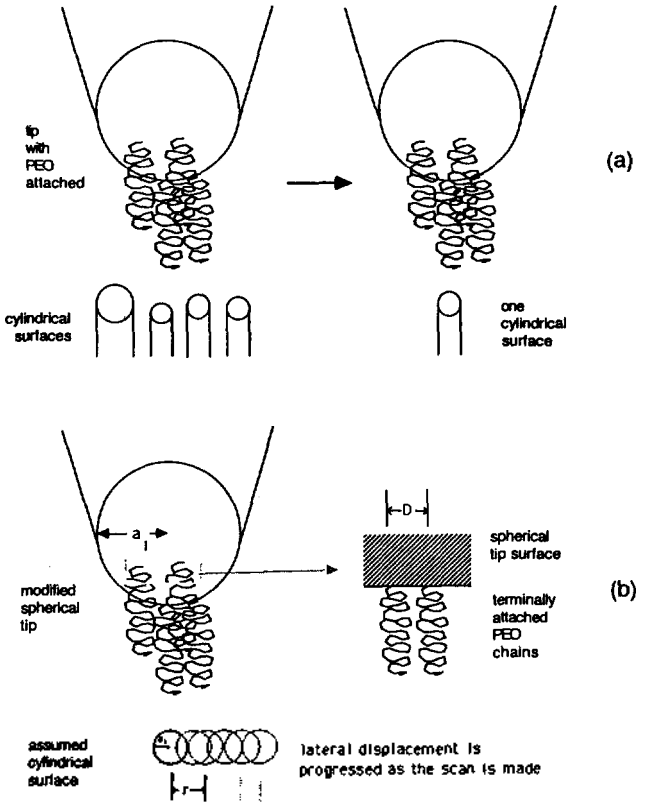

Figure 1. (a) Our model geometry, consisting of a spherical tip with terminally attached PEO chains and sample surface of cylindrical shapes. (b) One circular surface is moved laterally while the modified tip is fixed (scanning). The intermolecular forces between them are calculated as a function of the degree of lateral displacement of the circular surface, $r/2a_2$, where r is the distance from the original circular center to the displaced circular center and a_2 is the radius of sample surface of assumed circular shape. a_1 and D is the radius of assumed spherical tip and the distance between the terminally attached PEO chains, respectively.

only the long-range intermolecular forces between them (Figure 1(b)). The attached PEO chains exhibit steric repulsion force upon compression[19,20].

The crucial parameters are the distance D between the terminally attached PEO chains to the AFM tip, a measure of the surface chain density, the degree of polymerization, N, a measure of the chain length, the radius of circular surface, a_2, a measure of the size of adsorbed protein on mica, and the radius of spherical tip, a_1, a measure of the AFM tip size (Figure 1(b)). Only the "brush" case is considered[11].

Method

Considered long-range intermolecular forces in aqueous media for our modified AFM system are van der Waals and steric repulsion (electrostatic forces are ignored because of the attached neutral PEO chains[19,20]). The non-retarded van der Waals force between the large spherical AFM tip and one small circle surface across the terminally attached PEO media is given as[9]:

$$F(VDW) = -\pi a_2^2 \cdot \frac{A}{6\pi L^3} \quad (1)$$

where A is the Hamaker constant[19,20] between the AFM tip and protein adsorbed circle surface across a medium (PEO in water); a_2 is the radius of circular protein (πa_2^2 is the area); L is the separation distance between the spherical AFM tip and circular protein surface. The long-range repulsive steric force of the PEO-modified tip under the effect of circular protein is calculated as the steric repulsion force per unit surface area[13,19] multiplied by πa_2^2:

$$F(S) = \pi a_2^2 \cdot kT\frac{k_1}{a^2}\left(\frac{7}{5}\frac{k_2}{k_1}\right)^{5/12} N\sigma^{11/6}\left(\frac{5}{4}\frac{1}{L_0}\right)\left[\left(\frac{L_0}{L}\right)^{9/4} - \left(\frac{L}{L_0}\right)^{3/4}\right] \quad (2)$$

where k is the Boltzman constant; T is the absolute temperature; a is the monomer size of PEO (2.78 Å)[25,26]; N is the degree of polymerization; σ is the surface density of PEO ($\sigma = a^2/D^2$); L_0 is the theoretical equilibrium layer thickness of terminally attached chains in a good solvent system, $L_0 = (5/7 \cdot k_1/k_2)^{1/3} aN\sigma^{1/3}$; and the k_1 and k_2 are the osmotic and elastic contribution of PEO chains and given as 0.004 and 0.03, respectively, which are discussed in our previous paper[27].

We assume a minimum detectable force of 10^{-11} N[24,28], thus minimizing sample damage. To obtain the AFM detectable real long-range force, the attractive van der Waals force is added to the steric repulsion force. The individual and combined force ($F = F(VDW) + F(S)$) calculations were performed using N values from 50 to 150 and D values from 5 to 11 Å for the variation of separation distances between the spherical tip and one circular protein surface.

AFM scanning involves the lateral movement of the sample with respect to the tip[4,5,29]. If the separation distance between two centers increases, the interaction force between them is decreased (Figure 1(b)) (contant "height" method)[4,5,29]. The rate of the decrease of the force during a scan can affect the cantilever deflection, and the "resolution" of the image of one circular surface.

Results and Discussion

The larger steric repulsion forces are reduced by the attractive van der Waals forces. The combined force must be considered in the following text (the force means the combined force if without any remark). The combined force is also compared with the attractive van der Waals force (resulting from our bare AFM tip without any attached polymer chains). The increase of the forces above 10^{-11} N can damage the protein surface[24,28]. Maintaining the forces at about 10^{-11} N is important in AFM measurements without the damage of sample.

Separation distances between the tip and one circular surface, maintaining a force of 10^{-11} N, are calculated as a function of the circular surface area for different surface density and chain length of terminally attached PEO (Figure 2). To have the merit of using the steric repulsion forces of the modified AFM system compared with the unmodified ones, the spearation distances with maintaining the combined force at 10^{-11} N must be longer than those with the van der Waals force of 10^{-11} N (the tip must closely approach to the surface

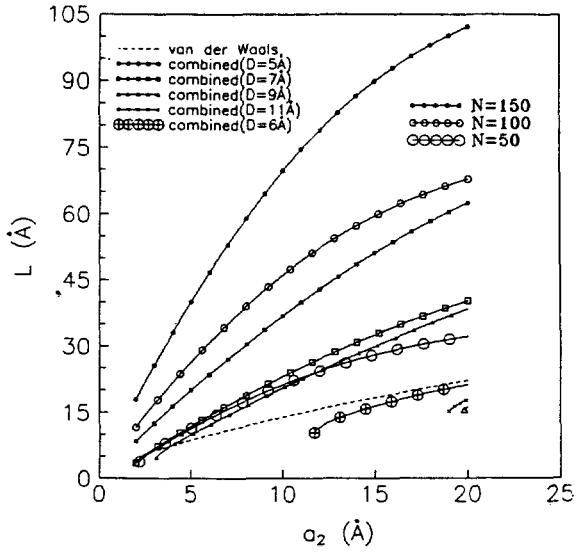

Figure 2. The separation distance, L, plotted against various sizes of circular surfaces for 2 different D values (5 and 6 Å) at $N=50$, 3 different D values (5, 7, and 9 Å) at $N=100$, and 4 different D values (5, 7, 9, and 11 Å) at $N=150$, maintaining a constant combined force of 10^{-11} N. The separation distances with maintaining a constant absolute value of van der Waals force of 10^{-11} N are also inserted for comparison.

of sample to detect the van der Waals force of 10^{-11} N, and then the tip can damage the surface[28]). It can be achieved by the increase of surface density and chain length of PEO attached to the AFM tip. The distance between the terminally attached PEO chains, D, above 5 Å must be considered because the surface density of crystalline PEO is 0.36[19,20,25,26]. The distances, D, longer than 6 Å for $N=50$, 9 Å for $N=100$, and 11 Å for $N=150$ produce a combined force lower than the absolute value of van der Waals force in our studied range of circular surface size, meaning the loss of steric repulsion concept under the assumption of only two long-range forces (steric and van der Waals). The distance between the terminally attached chains must be shorter (higher density) than the above critical values to have the combined force detectable at 10^{-11} N. The separation distances between the modified AFM tip and the sample surface increase with increase of observable protein surface size and the extent is greater at longer chain length of PEO. Maintaining forces of 10^{-11} N at longer separation distances can be obtained by higher surface density and longer chain length of PEO. This is desirable for AFM measurements because operation of AFM at shorter separation distances between the AFM tip and the circular surface can induce abrupt attraction of the tip to the substrate (the tip adheres strongly to the substrate end can be withdrawn only with difficulty), and can deform and distort the adsorbed protein surface[28,30,31]. The higher surface density of attached PEO is very difficult to obtain experimentally[12,32,33]. Longer chains with experimentally obtainable higher surface density of PEO must be attached to the AFM tip to get the larger steric repulsion forces at longer separation distances.

As the scan is made, the larger spherical tip with PEO is fixed and the smaller circular surface is moved laterally

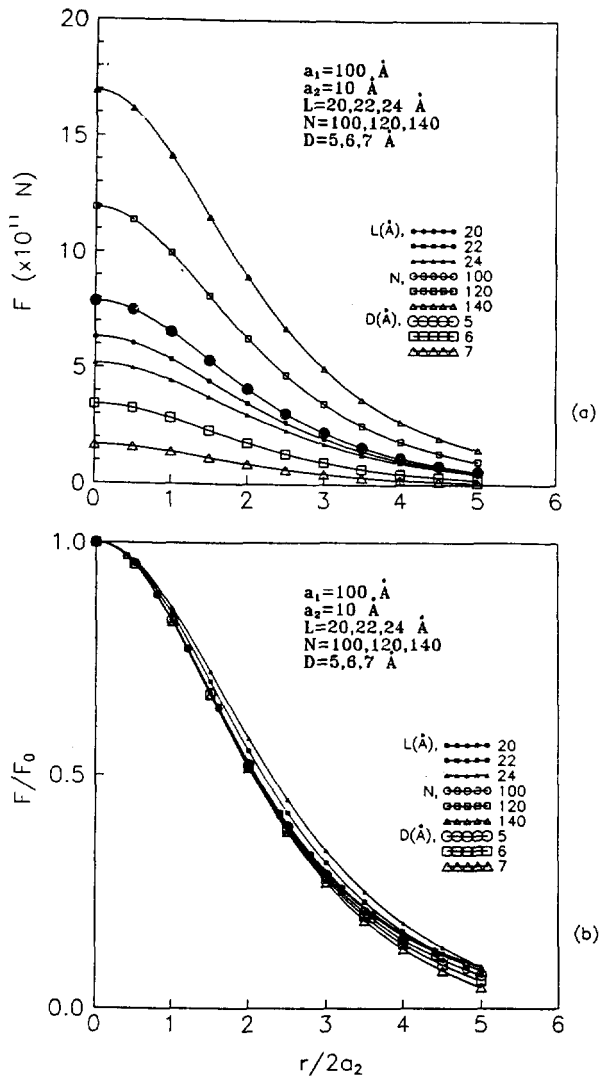

Figure 3. (a) The combined force F, and (b), its relative value, F/F_0, plotted against the lateral displacement of one circle, $r/2a_2$, for 3 different separation distances ($L=20$, 22, and 24 Å) at $N=100$ and $D=5$ Å, 3 different chain lengths ($N=100$, 120, and 140) at $L=20$ Å and $D=5$ Å, and 3 different surface density ($D=5$, 6, and 7 Å) at $L=20$ Å and $N=100$ as the scan is made. a_1 and a_2 are fixed at 100 Å and 10 Å, respectively. F, the force between tip and one circular surface at any lateral movement of the surface (during scanning) divided by, F_0, the starting force between tip and assumed center circular surface just under the tip (before scanning), *i.e.*, F/F_0, gives the relative value of the combined force.

under it, exhibiting gradually declining long-range intermolecular forces between them (Figure 1(b)). The combined long-range intermolecular forces are calculated as a function of the lateral movement of the circular surface from the tip, represented as $r/2a_2$, where r is the distance from the original circular center to the displaced circular center and a_2 is the radius of assumed single circular surface. First, we examine the effect of variation of the separation distance between the constant sizes of tip and circular surface, and the degree of polymerization and the surface density of attached PEO, to the combined intermolecular force (Figure

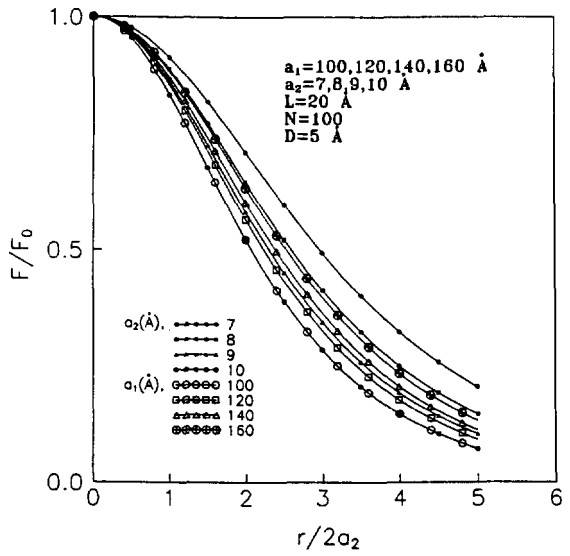

Figure 4. The relative value, F/F_0, plotted against $r/2a_2$ for 4 different sizes of assumed circular surface (a_2=7, 8, 9, and 10 Å) at a_1=100 Å and 4 different sizes of assumed spherical tip (a_1=100, 120, 140, and 160 Å) at a_2=10 Å. L, N, and D are fixed at 20 Å, 100, and 5 Å, respectively.

3(a)). The force is gradually decreased as the scan is made for all of our examined cases. To compare the extent of decreasing force for the lateral movement of the circular surface, the calculated force is expressed as a relative value, which affects the degree of cantilever deflection and gives a rough estimate of the "resolution" of surface image (Figure 3(b)). The difference of slopes is slight. The interested one is that the increase of chain length and surface density of PEO induces a larger increase of the force (Figure 3(a)), but the relative force has no profound difference (Figure 3(b)). Thus "resolution" is not affected, but the force is easier to detect by AFM. If the un-modified AFM cannot detect the smaller intermolecular force at some longer separation distance because of instrumental limitations, one must increase the detectable force by decrease of separation distance. The AFM can detect the larger force, but the closer approach of two surfaces (tip and sample surface) can induce attraction between them, perhaps deforming the surface[28,30,31]. All of these problems are alleviated with the modified AFM, obtained by increasing chain length and surface density of the attached PEO, allowing longer separation distances to be used.

A larger circular surface decreases the intermolecular force more steeply and can give a finer circle image (Figure 4), which may be a naturally occurring consequence. AFM tip size has also to be decreased at a fixed chain length and surface density of PEO to obtain a finer surface image *i.e.*, the smaller the tip size, the better the "resolution" (Figure 4).

Modified AFM tips to permit detectable force at relatively longer separation distances and with minimal sample surface deformation require the following conditions: longer chain length and maximal surface density of terminally attached PEO to the smallest possible AFM tip. The surface density is more important than chain length in maximizing the steric repulsion[19,20].

Conclusion

This study is based on the assumption of PEO chains terminally attached to a spherical AFM tip in aqueous media, interacting with one finite circular "protein" surface (*i.e.*, modified AFM system). Only two long-range intermolecular forces between the two surfaces are assumed: van der Waals attraction and steric repulsion. To obtain an estimate of the total force detected by the AFM, the two individual forces are combined. The combined forces are calculated as a function of surface density and chain length of PEO, as well as other variables, and compared with the absolute values of the van der Waals force to obtain the use of long-range steric repulsion force. To get the AFM detectable combined force of 10^{-11} N at relatively longer separation distance, an increase in surface density and chain length of PEO is necessary. The best conditions for N=50, N=100, and N=150 require the chains on the surface to be less than 6, 9, and 11 Å apart, respectively. The intermolecular forces between the spherical AFM tip and one circular protein surface decrease with an increase in separation distance. The longer separation distances, while maintaining forces of 10^{-11} N (which minimally deform the "protein" surface and are more desirable for AFM), can be obtained by higher surface density and longer chain length of PEO. The variation of surface density and chain length of PEO affects the magnitude of the steric repulsion force, but does not significantly affect the "resolution". "Resolution" is improved by the decrease of tip size.

Acknowledgement. This paper was supported (in part) by NON DIRECTED RESEARCH FUND, Korea Research Foundation, 1991 and one of the authors (SIJ) also thanks to the Natural Science Research Institute at Kangnung National University.

References

1. G. Binning, C. F. Quate, and Ch. Gerber, *Phys. Rev. Lett.*, **56**, 930 (1986).
2. P. K. Hansma, V. B. Elings, O. Marti, and C. E. Bracker, *Science*, **242**, 209 (1988).
3. J. N. Lin, B. Drake, A. S. Lea, P. K. Hansma, and J. D. Andrade, *Langmuir*, **6**, 509 (1990).
4. B. Drake, C. B. Prater, A. L. Weisenhorn, S. A. C. Gould, T. R. Albrecht, C. F. Quate, D. S. Canneli, H. G. Hansma, and P. K. Hansma, *Science*, **243**, 1586 (1989).
5. G. Friedbacher, P. K. Hansma, E. Ramli, and G. D. Stucky, *Science*, **253**, 1261 (1991).
6. J. H. Hoh, R. Lal, S. A. John, J.-P. Revel, and M. F. Arnsdorf, *Science*, **253**, 1405 (1991).
7. O. M. Leung and M. C. Goh, *Science*, **255**, 64 (1992).
8. A. S. Lea, A. Pungor, V. Hlady, J. D. Andrade, J. N. Herron, and E. W. Voss, Jr., *Langmuir*, **8**, 68 (1992).
9. J. N. Israelachvili, "Intermolecular and Surface Forces", Academic Press, London, 1985.
10. W. A. Ducker, T. J. Senden, and R. M. Pashley, *Nature*, **353**, 239 (1991).
11. P. G. de Gennes, *Ann. Chim.*, **77**, 389 (1987).
12. H. J. Taunton, C. Toprakcioglu, L. J. Fetters, and J. Klein,

Nature, **332**, 712 (1988).
13. S. Patel, M. Tirrell, and G. Hadziioannou, *Colloids and Surfaces*, **31**, 157 (1988).
14. D. E. Gregonis, D. E. Buerger, R. A. Van Wagenen, S. K. Hunter, and J. D. Andrade, *Biomaterials 84, Trans. Soc. Biomaterials*, **7**, 766 (1984).
15. J. D. Andrade ed., "Surface and Interfacial Aspects of Biomedical Polymers", Ch. 1, Plenum Press, NY, 1985.
16. J. D. Andrade, S. Nagaoka, S. Cooper, T. Okano, and S. W. Kim, *ASAIO J.*, **10**, 75 (1987).
17. J. H. Lee, "Interactions of PEO-containing Polymeric Surfactants with Hydrophobic Surfaces", Ph. D. Thesis, University of Utah, 1988.
18. W. R. Gombotz, A. S. Hoffman, J. M. Harris, B. Hovanes, G. H. Wang, and A. Safranj, IUPAC-Macromolecules Symposium, Seoul, Korea, June 1989.
19. S. I. Jeon, J. H. Lee, J. D. Andrade, and P. G. de Gennes, *J. Colloid Interface Sci.*, **142**, 149 (1991).
20. S. I. Jeon and J. D. Andrade, *J. Colloid Interface Sci.*, **142**, 159 (1991).
21. P. G. de Gennes, "Scaling Concepts in Polymer Physics", Cornell University Press, Ithaca, 1979.
22. P. G. de Gennes, *Macromolecules*, **14**, 1637 (1981).
23. P. G. de Gennes, *Macromolecules*, **15**, 492 (1982).
24. B. N. J. Persson, *Chem. Phys. Letters*, **141**, 366 (1987).
25. H. Tadokoro, Y. Chatani, T. Yoshihara, S. Tahara, and M. Murahashi, *Macromol. Chem.*, **73**, 109 (1964).
26. Y. Takahashi and H. Tadokoro, *Macromolecules*, **6**, 672 (1973).
27. S. I. Jeon and J. D. Andrade, *Bull. Korean Chem. Soc.*, **13**, 245 (1992).
28. U. Hartmann, to be published.
29. S. I. Jeon and J. D. Andrade, to be published.
30. H. G. Hansma, J. Vesenka, C. Siegerist, G. Kelderman, H. Morrett, R. L. Sinsheimer, V. Elings, C. Bustamante, and P. K. Hansma, *Science*, **256**, 1180 (1992).
31. C. Bustamante and J. Vesenka, *Polymer Preprints (ACS)*, **31**, 743 (1992).
32. J. Klein and P. F. Luckham, *Nature*, **300**, 429 (1982).
33. P. F. Luckham and J. Klein, *Macromolecles*, **18**, 721 (1985).

Molecular Dynamics Simulation Studies of Zeolite-A. II. Structure and Dynamics of Cations in Dehydrated Ca^{2+}-Exchanged Zeolite-A

Gyeong Keun Moon, Sang Gu Choi†, Han Soo Kim‡, and Song Hi Lee*

Department of Chemistry, Kyungsung University, Pusan 608-736
†Department of Industrial Safety, Yangsan Junior College, Yangsan 626-800
‡Department of Industrial Chemistry, Kangnung National University, Kangnung 210-702
Received November 4, 1992

In a recent paper[1] we reported molecular dynamics (MD) simulation of Na^+ ions in a rigid dehydrated zeolite-A framework at several temperatures using a simple Lennard-Jones potential plus Coulomb potential with Ewald summation to investigate the structure and dynamics of Na^+ ions. In this paper the same technique is applied to study the structre and dynamics of cations in dehydrated Ca^{2+}-exchanged zeolite-A systems, Ca_6-A and Ca_4Na_4-A. At 298.15 K the calculated positions of Ca^{2+} and Na^+ ions are in poor agreement with those determined by X-ray diffraction experiments, but this is reasonably explained by large repulsive interactions between cations. A simple harmonic oscillation of Ca^{2+} ions in dehydrated Ca_6-A zeolite and simultaneous random motions for the the same kinds of cations in dehydrated Ca_4Na_4-A zeolite due to a positional symmetry are observed in their velocity auto-correlation functions and mean square displacements. MD simulations of the fictitious Ca_8-A zeolite confirm our result for the behavior of Ca^{2+} ions in dehydrated Ca_6-A zeolite.

Introduction

In a previous paper (referred to Ref. 1 throughout this paper), we discussed a molecular dynamics (MD) simulation study of 12 Na^+ ions in rigid dehydrated zeolite-A framework. This study was carried out by the use of Ewald summation technique for the long-ranged character of Coulomb interaction. Our attention was mainly confined to the determination of a best-fitted set of interatomic potential parameters which include Lennard-Jones potential parameters and electrostatic charges of Na^+ ions and framework atoms. The next attention was given in the investigation of dynamic behavior of Na^+ ions at 298.15 K and 600.0 K using the previously determined interatomic potential parameters. Continuing that study here, we discuss new results in dehydrated, fully and partially, Ca^{2+}-exchanged zeolite-A. We have also extended our earlier techniques of MD simulation and Ewald summation to this study of dehydrated Ca_6-A and